

# Low mass planet migration in Hall-affected disks

Colin P McNally,<sup>1</sup> Richard P Nelson,<sup>1</sup> Sijme-Jan Paardekooper,<sup>1,3</sup>  
Oliver Gressel<sup>4</sup> and Wladimir Lyra<sup>5,6</sup>

<sup>1</sup> Astronomy Unit, School of Physics and Astronomy, Queen Mary University of London,  
London E1 4NS, UK

<sup>3</sup> DAMTP, University of Cambridge, Wilberforce Road, Cambridge CB3 0WA, UK

<sup>4</sup> Niels Bohr International Academy, The Niels Bohr Institute, Blegdamsvej 17, DK-2100,  
Copenhagen Ø, Denmark

<sup>5</sup> Department of Physics and Astronomy, California State University Northridge, 18111  
Nordhoff St, Northridge, CA 91330, USA

<sup>6</sup> Jet Propulsion Laboratory, California Institute of Technology, 4800 Oak Grove Drive,  
Pasadena, CA 91109, USA

E-mail: c.mcnally@qmul.ac.uk

**Abstract.** Recent developments in non-ideal magnetohydrodynamic simulations of protoplanetary disks suggest that instead of being traditional turbulent (viscous) accretion disks, they have a largely laminar flow with accretion driven by large-scale wind torques. These disks are possibly threaded by Hall-effect generated large-scale horizontal magnetic fields. We have examined the dynamics of the corotation region of a low mass planet embedded in such a disk and the evolution of the associated migration torque. These disks lack strong turbulence and associated turbulent diffusion, and the presence of a magnetic field and radial gas flow presents a situation outside the applicability of previous corotation torque theory. We summarize the analytical analysis of the corotation torque, give details on the numerical methods used, and in particular the relative merits of different numerical schemes for the inviscid problem.

## 1. Introduction

Protoplanetary disks, the formation sites of solar systems, are comprised of a very low ionization gas and a mixture of dust, boulders, and protoplanets. Simulations have shown that if the disk is threaded by a weak net vertical field, the disk develops an essentially laminar flow, as the magnetorotational instability is quenched by large Ohmic and Ambipolar diffusion. The spatial arrangement of these regimes is sketched in Figure 1. The accretion is driven by a wind from the most ionized region near the disk surfaces [1, 2]. Near the disk midplane, where Ohmic diffusion dominates, a ‘dead zone’ forms ( $0.5 \lesssim R \lesssim 10$  au from the star), but at the same time the large Hall effect can give rise to strong fields when the background field is aligned with the disk rotation [3, 4]. These laminar magnetic fields can give rise to significant accretion at the midplane [1, 5, 6]. Recently in [7] we considered the problem of low mass planet migration in such a wind-driven protoplanetary disk that support accretion at the midplane [1, 5, 6, 8–14]. In this proceeding we summarize the problem and discuss the numerical issues in greater detail.

To study the flow near a low mass planet, we adopt a common two-dimensional formulation of the disk-planet interaction, and reduce the Hall-generated field to this dimensionality. In [7]

we find a equilibrium field for the unperturbed disk:

$$B_r = B_0 \left( \frac{r}{r_0} \right)^{-1} \quad B_\phi = -2B_0 \Omega_0 r_0^2 \frac{\mu_0}{\eta} \left( \frac{r}{r_0} \right)^{-1/2} \quad (1)$$

where  $B_r$  and  $B_\phi$  are the radial and azimuthal magnetic fields,  $r$  is the cylindrical radius,  $r_0$  is a fiducial radius,  $\Omega_0$  is the Keplerian orbital frequency at  $r_0$ ,  $\eta$  is the Ohmic resistivity, and  $\mu_0$  the vacuum permeability. This magnetic field drives radial motion of the disk gas at a velocity denoted  $v_r$ . Importantly, the resistivity of the dead zone region we study is very high, such that the timescale for magnetic field perturbations to diffuse across the length scale of interest (the planet's corotation region) is very small compared to the timescale for fluid elements to make the horseshoe turn at the end of a librating orbit in that corotation region. So, although the disk is well enough ionized so that the magnetic field drives the radial motion of the disk gas, the magnetic field response to the presence of the planet may be very small. Indeed, upon investigation we found it to be negligible.

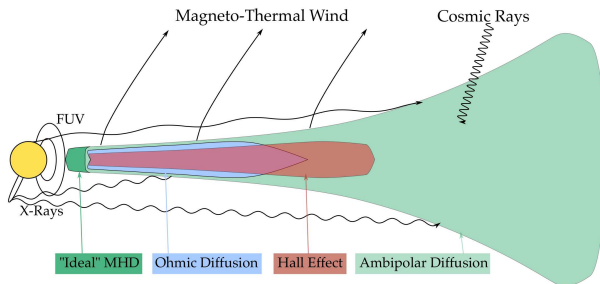


**Figure 1.** Schematic of the structure of a wind-driven protoplanetary disk in terms of ionization sources and non-ideal MHD terms.

## 2. Corotation Torques

When a low mass planet is placed in a disk, the response of the disk to this perturbation creates under- and over-densities. These density perturbations gravitationally tug on the planet in the form of a torque which modifies its orbit. Here, we focus exclusively on the corotation torque, arising from perturbations in the coorbital region, and for brevity neglect discussion of the spiral wave and associated Lindblad torque as they are not modified by the magnetic field in this case. In this section we summarize the theory for the corotation torque arising in this inviscid flow by considering the magnetic field as a fixed body force acting on the gas. The presentation is a brief summary of the analytical results of [7].

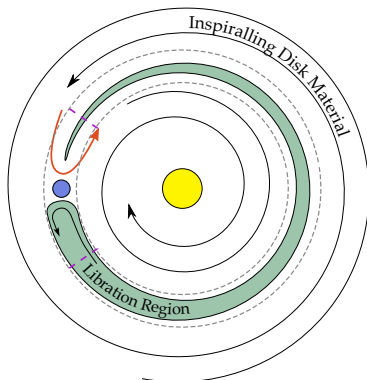


**Figure 2.** Cartoon of the flow in and around the corotation region of a low mass planet in a magnetically torqued dead zone. The magnetic torque drives disk gas inwards, and distorts the island of librating material (green) into an asymmetrical tadpole-like shape. This asymmetry of the librating material, and the introduction of the flow-through stream (red) lead to the corotation torque.

In our disk with a laminar magnetic field driving accretion, the laminar flow past the planet is illustrated in Figure 2. Disk gas spirals inwards as it loses angular momentum to the magnetic field. When it encounters the planet from the outside it executes a turn, giving angular momentum to the planet and making a quick jump inwards toward the star. The width of the turn is  $2x_s$ , where  $x_s$  is the half-width of the corotation region. Within the corotation region, there is gas that is trapped on librating orbits. These orbits execute two horseshoe turns, in front and behind of the planet. Due to the action of the magnetic field these orbits are also asymmetrical, as the gas drifts radially inwards between turns. Thus, on the turn in front of the planet, both gas flowing through the coorbital region and gas on librating orbits makes the turn. In the turn behind the planet, only gas on librating orbits makes the turn. The difference between the rate of angular momentum exchange with the planet by the gas on these two turns gives rise to the corotation torque.

To isolate the corotation torque due to the radial gas flow, and remove thermal effects (the entropy-related torque), we employ a globally isothermal disk with power law surface density  $\Sigma = \Sigma_0 (r/r_0)^{-\alpha}$ . In [7] we show that the corotation torque can be calculated in terms of the inverse vortensity  $w = \Sigma/\nabla \times \mathbf{v}$  of the material undergoing the two horseshoe turns. Due to the steady-state magnetic accretion stress in the disk, as gas spirals inwards, the value of the vortensity at any given radial location in the flow is constant, even though the vortensity of a given fluid element increases as it moves inwards. At the same time, the gas in the libration region has constantly increasing vortensity because the same Lorentz force acts on it but it is not free to fall inwards towards the star. The analysis in [7] yields the expression for the torque associated with these two horseshoe turns

$$\Gamma_{\text{hs}} = 2\pi \left( 1 - \frac{w_c(t)}{w(r_p)} \right) \Sigma_p r_p^2 x_s \Omega_p (-v_r), \quad (2)$$

where  $w(r_p)$  is the inverse vortensity of the unperturbed disk at the planet location,  $w_c(t)$  is the time-evolving characteristic value of the inverse vortensity in the libration region,  $\Omega$  is the orbital frequency of the disk,  $x_s$  is the corotation region half width, and quantities at the planet position are denoted with a subscript  $p$ . The corotation region half width for a low mass planet is approximately  $x_s = 1.2r_p \sqrt{(q/h)}$  where  $q$  is the planet-star mass ratio, and  $h = H/r$  is the non-dimensional pressure scale height. For the purposes of this discussion, we give the evolution of  $w_c$  in a simple form as

$$w_c(t) = w(r_p) [1 + t/\tau_w]^{-1}, \quad \tau_w = \left[ \left( \frac{3}{2} - \alpha \right) \frac{(-v_r)}{r_p} \left( \frac{r_p}{r_0} \right)^{\alpha - \frac{5}{2}} \right]^{-1}. \quad (3)$$

The full development of this formula, analysis of relevant timescales and its applicability are discussed in [7].

From this discussion of the analytical approach to the problem, we can see that to arrive at good numerically approximated solutions to this inviscid problem we require that the vortensity of the material trapped in the libration region should not artificially mix with the flow-through material, so that the evolution of  $w_c(t)$  is correctly obtained. This becomes the main criteria for successfully running a fluid simulation.

### 3. Methods for full magnetohydrodynamics

The first code the problem was attacked with was NIRVANA3.5 [15, 16]. As employed here, it is a second order accurate Godunov method, with an HLLD Riemann solver and a CTU scheme for the magnetic field evolution and second-order Runge-Kutta time integration. Because of the very large Ohmic diffusion, the parabolic term is treated with a Runge-Kutta-Legendre

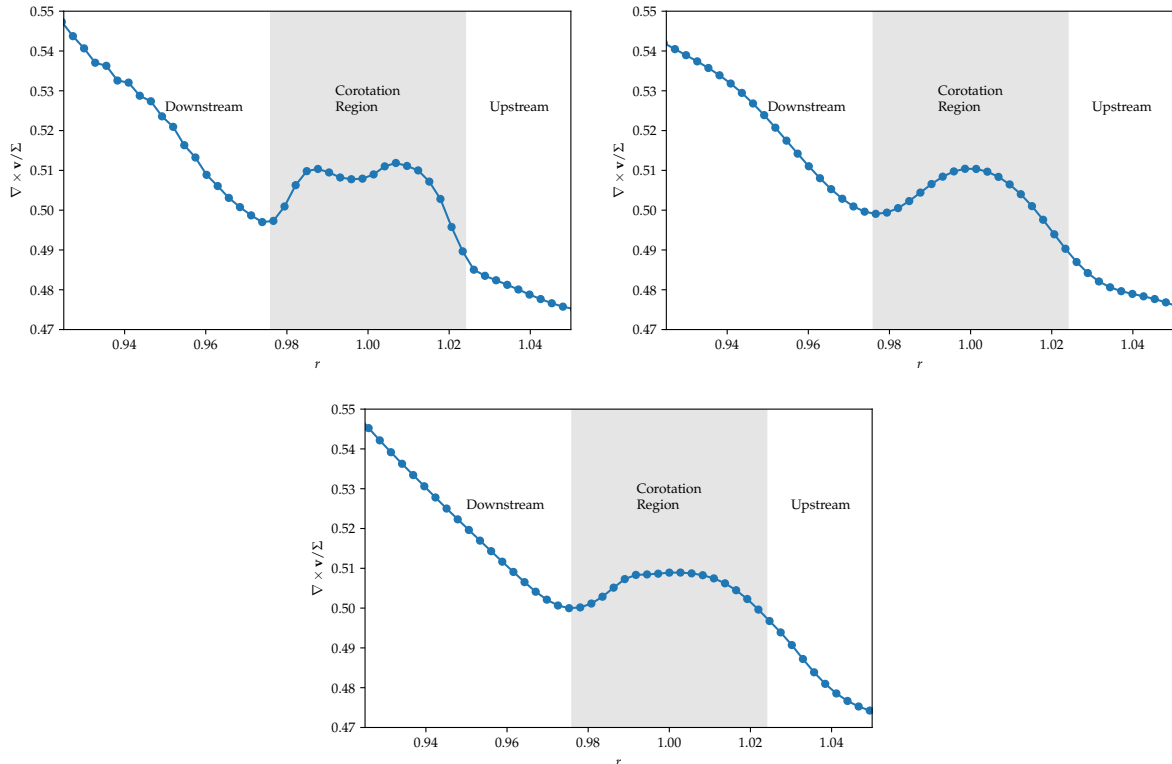


**Figure 3.** Illustration of the difference between simulations in three codes. Examples of the vortensity perturbation in the corotation region, in a radial cut opposite to the planet after 240 orbits at a low resolution as specified in the text. Upper Left: FARGO3D, Upper Right: The PENCIL CODE, Lower Center: NIRVANA3.5

polynomial based second-order accurate super-time-stepping scheme (RKL2) [17], as previously employed in [2]. In addition, we have newly implemented a conservative orbital advection scheme following [18], employing a FFT-based spectral interpolation for the azimuthal advection.

Typically, we find that the super-time-stepping allows a time step  $\sim 2000$  times greater than the stability limit for a basic explicit finite difference integration of the diffusion operator, by employing a super time stepping solver with  $\sim 65$  stages on each stage of the two-stage Runge-Kutta hydrodynamics time step with a wall clock speed-up of  $\sim 17$  times over a simple explicit integration. The RKL2 super time stepping scheme displayed no instability despite these extreme time step ratios. Moreover, through these experiments we find that the problem can be described well by fixing the magnetic field and neglecting the induction equation. This allowed the problem to be described as one in pure isothermal hydrodynamics, with a simple body force added to describe the Lorentz force from the magnetic field [7]. Thus we were able to progress with a simplified problem, and search for even more efficient codes for this problem.

#### 4. The fixed magnetic field problem and vortensity evolution

The PENCIL CODE [19, 20] is a high-order finite difference method based on point collocation values and sixth-order centered differences in space to construct a method-of-lines approach to the MHD equations and applying a third-order time integration scheme. In addition, for disk problems like the one here, we have implemented an orbital advection technique by splitting of the time integration [21], without decomposing the velocity field as in NIRVANA.

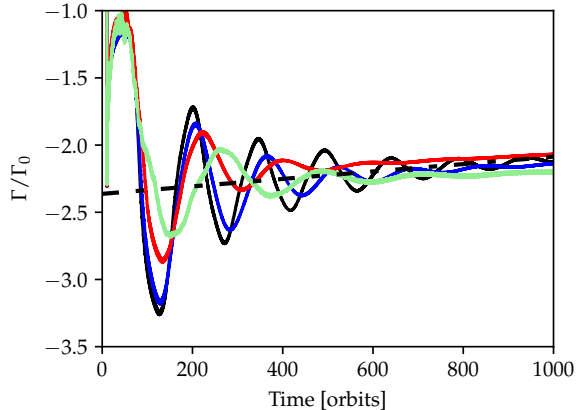


**Figure 4.** Convergence of torque histories from FARGO3D simulations and the analytical prediction. Grid resolutions are doubled between each run, with the sequence light green, red, blue, black, and the analytical formula equation (2) is plotted with a dashed line. The total torque  $\Gamma$  is scaled by  $\Gamma_0 = (q/h)^2 \Sigma_p r_p^4 \Omega_p^2$ .

With this technique, the bulk azimuthal advection due to Keplerian motion is achieved with a FFT-based spectral interpolation, yielding a significant speedup and lower numerical diffusion while preserving the third order accuracy in time on the integration scheme. Stability for the integration scheme is achieved by modifying the governing equations with the addition of diffusion operators. The usual minimal choices in the PENCIL CODE for a problem like the one at hand are a hyperdiffusion of the form  $\nabla^6 = \nabla^2(\nabla^2(\nabla^2))$  applied to all fields to stabilize the grid scale, and a shock-viscosity. The full form of the hyperdiffusion operator and the scaling of the hyperdiffusion coefficient as applied in cylindrical coordinates is given in the appendix of [21]. Importantly, this hyperdiffusion has shear components which can mix vortensity into the libration region at the grid scale.

FARGO3D [22–24] is based on an operator splitting technique with a second-order conservative finite differences in space. However, to gain stability the scheme employs only a bulk shock-viscosity with no shear components. Additionally, the method is known to have good properties for the conservation and advection of vortensity ( $\nabla \times \mathbf{v}/\Sigma$ ) [23]. Although the PENCIL CODE has a high formal order of accuracy and has excellent fidelity for quickly evolving shear flow problems [25], for this problem the slow formation (hundreds of orbits) of the vortensity structure in the corotation region is washed out by the shear component of the stabilizing hyperdiffusion. Thus, although it has a lower formal order of accuracy, we found FARGO3D to be efficient in practice for achieving solutions with approximately the correct physical properties, particularly the sharp, relatively undiffused vortensity profile shown in Figure 3. This comparison uses a cylindrical grid of 512 zone in radius and 1536 in azimuth, with a radial range [0.3, 1.7] and boundary conditions and planet potential as employed in [7]. The planet/star mass ratio was  $2 \times 10^{-5}$ . In the PENCIL CODE the `hyper3-cyl` [21] diffusions of velocity and density were employed with the coefficient set to  $10^{-4}$ , the smallest value found to yield stability. In addition, the shock-capturing artificial viscosity `nu-shock` was employed on the velocity field with the coefficient set to 1. In this comparison, NIRVANA3.5 solved only hydrodynamics with the magnetic force replaced by a body force as in the other codes, and the monotonized central slope limiter was selected. In agreement with previous commentary on Godunov methods [23] for similar problems, we found that the algorithm we applied in NIRVANA3.5 diffused the sharp vortensity profile in the corotation region more than FARGO3D. We note that the choice of limiter does have a significant effect on the numerical diffusion of vortensity in that method. With higher resolution versions of these FARGO3D simulations, we were able to verify our analytical prediction for the corotation torque, as shown by the example in Figure 4.

## 5. Conclusions

In summary, we have:

- Implemented orbital advection schemes appropriate for disk problems in NIRVANA3.5 and the PENCIL CODE
- Demonstrated the practical application of RKL2 super time stepping for Ohmic resistivity to very diffusive setups with no numerical stability issues arising
- Described the relative strengths of the main methods used in NIRVANA3.5, the PENCIL CODE, and FARGO3D, all well-proven and high-quality codes in their own rights, for an inviscid disk problem where evolution of vortensity is paramount, finding the best results with FARGO3D
- Developed a torque formula for the corotation torque on a low mass planet embedded in a magnetically torqued dead zone

## Acknowledgments

This research was supported by STFC Consolidated grants awarded to the QMUL Astronomy Unit 2015-2018 ST/M001202/1 and 2017-2020 ST/P000592/1. The simulations presented in this paper utilized Queen Mary's MidPlus computational facilities, supported by QMUL Research-IT and funded by EPSRC grant EP/K000128/1; the DiRAC Complexity system, operated by the University of Leicester IT Services, and the DiRAC Data Centric system at Durham University, operated by the Institute for Computational Cosmology which form parts of the STFC DiRAC HPC Facility ([www.dirac.ac.uk](http://www.dirac.ac.uk)). This equipment is funded by BIS National E-Infrastructure capital grants ST/K000373/1, ST/K00042X/1; STFC capital grant ST/K00087X/1, and STFC DiRAC Operations grants ST/K0003259/1 and ST/K003267/1. DiRAC is part of the National E-Infrastructure. This work used the NIRVANA3.5 code developed by Udo Ziegler at the Leibniz Institute for Astrophysics (AIP). This research was supported in part by the National Science Foundation under Grant No. NSF PHY11- 25915. The research leading to these results has received funding from the European Research Council (ERC) under the European Unions Horizon 2020 research and innovation programme (grant agreement No 638596). SJP is supported by a Royal Society University Research Fellowship.

## References

- [1] Bai X N and Stone J M 2013 ApJ **769** 76 (*Preprint* 1301.0318)
- [2] Gressel O, Turner N J, Nelson R P and McNally C P 2015 ApJ **801** 84 (*Preprint* 1501.05431)
- [3] Wardle M and Ng C 1999 MNRAS **303** 239–246 (*Preprint* astro-ph/9810468)
- [4] Pandey B P and Wardle M 2008 MNRAS **385** 2269–2278 (*Preprint* 0707.2688)
- [5] Lesur G, Kunz M W and Fromang S 2014 A&A **566** A56 (*Preprint* 1402.4133)
- [6] Béthune W, Lesur G and Ferreira J 2017 A&A **600** A75 (*Preprint* 1612.00883)
- [7] McNally C P, Nelson R P, Paardekooper S J, Gressel O and Lyra W 2017 MNRAS **472** 1565–1575 (*Preprint* 1708.05721)
- [8] Bai X N 2013 ApJ **772** 96 (*Preprint* 1305.7232)
- [9] Bai X N 2014 ApJ **791** 73
- [10] Bai X N 2014 ApJ **791** 137 (*Preprint* 1402.7102)
- [11] Bai X N 2015 ApJ **798** 84 (*Preprint* 1409.2511)
- [12] Simon J B, Lesur G, Kunz M W and Armitage P J 2015 MNRAS **454** 1117–1131 (*Preprint* 1508.00904)

- [13] Bai X N, Ye J, Goodman J and Yuan F 2016 ApJ **818** 152 (*Preprint* 1511.06769)
- [14] Bai X N 2016 ApJ **821** 80 (*Preprint* 1603.00484)
- [15] Ziegler U 2004 *Journal of Computational Physics* **196** 393–416
- [16] Gressel O 2017 Toward realistic simulations of magneto-thermal winds from weakly-ionized protoplanetary disks *Journal of Physics Conference Series (Journal of Physics Conference Series* vol 837) p 012008 (*Preprint* 1611.09533)
- [17] Meyer C D, Balsara D S and Aslam T D 2012 MNRAS **422** 2102–2115
- [18] Mignone A, Flock M, Stute M, Kolb S M and Muscianisi G 2012 A&A **545** A152 (*Preprint* 1207.2955)
- [19] Brandenburg A and Dobler W 2002 *Computer Physics Communications* **147** 471–475 (*Preprint* astro-ph/0111569)
- [20] Brandenburg A and Dobler W 2010 Pencil: Finite-difference Code for Compressible Hydrodynamic Flows Astrophysics Source Code Library (*Preprint* 1010.060)
- [21] Lyra W, McNally C P, Heinemann T and Masset F 2017 AJ **154** 146 (*Preprint* 1708.05057)
- [22] Benítez-Llambay P and Masset F S 2016 ApJS **223** 11 (*Preprint* 1602.02359)
- [23] Masset F S and Benítez-Llambay P 2015 Planet-Disk Interaction on the GPU: The FARGO3D code *Numerical Modeling of Space Plasma Flows ASTRONUM-2014 (Astronomical Society of the Pacific Conference Series* vol 498) ed Pogorelov N V, Audit E and Zank G P p 216
- [24] Masset F 2000 A&AS **141** 165–173 (*Preprint* astro-ph/9910390)
- [25] McNally C P, Lyra W and Passy J C 2012 ApJS **201** 18 (*Preprint* 1111.1764)